

$^{15}\text{O}+\alpha$ resonant elastic scattering to study cluster states in ^{19}Ne

D Torresi¹, C Wheldon¹, Tz Kokalova¹, S Bailey¹, A Boiano², C Boiano³, M Cavallaro⁴, S Cherubini⁴, A Di Pietro⁴, J P Fernandez Garcia⁴, M Fisichella⁴, T R Glodariu⁵, J Grebosz⁶, M La Cognata⁴, M La Commara^{2,7}, M Lattuada^{4,8}, M Mazzocco^{9,10}, D Mengoni^{9,10}, C Parascandolo^{2,7}, D Pierroutsakou⁴, G Pizzone^{4,8}, C Signorini¹⁰, C Stefanini⁹, L Stroe⁵, C Spitaleri^{4,8}, E Strano^{9,10} and M Zadro¹²

¹School of Physics, University of Birmingham, Birmingham, B15 2TT, UK

²INFN-Sezione di Napoli, Via Cinthia, I-80126 Napoli, Italy

³INFN-Sezione di Milano, Via Celoria 16, I-20133 Milano, Italy

⁴INFN-Laboratori Nazionali del Sud, Via S. Sofia 62 Catania, Italy

⁵TNIPNE, 407 Atomistilor Street, 077125 Magurele, Romania

⁶Department of Nuclear Reactions, Institute for Nuclear Studies, ul. Hoza 69, 00-681 Warsaw, Poland

⁷Dipartimento di Fisica, Università di Napoli, Via Cinthia, I-80126 Napoli, Italy

⁸Dipartimento di Fisica, Università di Catania, Via A. Doria 64, I-95123 Catania, Italy

⁹INFN-Sezione di Padova, Via F. Marzolo 8, I-35131 Padova, Italy

¹⁰INFN-Laboratori Nazionali di Legnaro, Viale dell'Università 2, I-35020 Legnaro, Italy

E-mail: domenico.torresi@lns.infn.it

Abstract. Clustering phenomena are well known in nuclear physics for stable nuclei, both α -conjugate ($N=Z$, $A=2N$), like ^8Be , ^{16}O , ^{20}Ne , and non- α -conjugate, like ^6Li and ^7Li . In general, it is expected that light exotic nuclei may also exhibit cluster behavior. Moving out of the valley of stability configurations can be found where at least one of the clusters is unbound or weakly bound, thus not satisfying the strong internal correlation requirement of classical clusters. This is so-called exotic clustering. The study of such systems presents many difficulties, due, mainly, to the low intensities typical of radioactive ion beams. Therefore, few significant experimental studies have been performed so far. In this work we searched for α -cluster states in ^{19}Ne above its α -decay threshold measuring, for the first time, the $^{15}\text{O}(^4\text{He},^4\text{He})$ elastic scattering excitation function. Moreover, this study classified low-energy states in Ne in the astrophysically important region in this HCNO-break-out nucleus.

1. Introduction

In recent years the isotope ^{19}Ne has attracted much interest. This is mainly due to the astrophysical importance of the $^{15}\text{O}(\alpha,\gamma)^{19}\text{Ne}$ reaction rate that was identified as a break out from the hot-CNO cycles and a trigger for the following rapid proton capture that populate masses higher than neon [1]. Therefore, the structure of the low-energy spectrum of ^{19}Ne close to the $^{15}\text{O}+\alpha$ threshold ($S_\alpha=3.528$ MeV) is very important. Moreover, the states in ^{19}Ne near the proton threshold ($S_p=6.411$ MeV), are again important, as the destruction of the key radio-nuclide ^{18}F [2], occurs mainly via the $^{18}\text{F}(p,\alpha)^{15}\text{O}$ reaction.



Neon isotopes exhibit strong α -clustering phenomena, even in the ground states. Neon-20 [3, 4, 5] and ^{21}Ne [6, 7] are two of the best examples of nuclear clustering known to date. Therefore, it is important to extend this cluster study to the neutron poor side of the neon isotopes that is, at the moment, almost totally unknown concerning the clustering point of view. This is needed in order to understand if such clustering phenomena persist in ^{19}Ne and, if so, to what extent. The present work reports the direct measurement of $^{15}\text{O}+\alpha$ elastic scattering using the technique of Thick Target Inverse Kinematics scattering [8] to investigate the structure of the low-lying-energy levels of ^{19}Ne . The method as implemented here allows the elastic scattering excitation function to be measured and enables to measure the α reduced α -width *directly* across a large excitation-energy range using a single beam energy. The nature of the technique makes it ideally suited to use with low-intensity, large-energy-profile radioactive ion beams.

2. The Experimental Technique

The TTIK method [9, 8, 10] with a gas target consists of delivering the beam into a reaction chamber filled with gas (typically ^4He) at such a pressure as to fully stop the beam. At the same time the gas acts as both target and degrader of the beam energy. The interaction between projectile and target nuclei can occur at different depths in the chamber along the beam direction, and thus at different energies. Thanks to the different stopping power of the gas for heavy projectiles and light recoils, the light recoiling particles can reach the telescopes placed at the downstream end of the chamber with respect to the entrance window. From the measurement of the recoil energy one can deduce the interaction position along the beam direction and thus the energy of the scattering event. This relationship is unequivocal if the detected light recoils originate from elastic scattering. The α -particles are detected at small angles covering the 0° region in the laboratory system, corresponding to the region around 180° in the center-of-mass. In this condition it is possible to extract the elastic scattering angular distribution in the region where the Coulomb scattering is minimized over the resonant elastic scattering. This technique is particularly suitable for measuring elastic scattering excitation functions with radioactive beams since it strongly reduces the beam time request with respect to the thin target technique.

2.1. The Experimental Apparatus

The ^{15}O radioactive ion beam was delivered by the EXOTIC facility [11, 12] at the Laboratori Nazionali di Legnaro (LNL, Italy) by means of the in-flight technique. A primary 80 MeV $^{15}\text{N}^{5+}$ beam was delivered by the LNL-XTU tandem Van de Graaff accelerator and impinged on a H_2 cryogenic gas target at a pressure of 1 bar and a temperature of 24° , corresponding to an equivalent target thickness of about 1.35 mg/cm^2 of H_2 . The ^{15}O beam [13], produced by means of the two-body reaction $p(^{15}\text{N}, ^{15}\text{O})n$ ($Q_{\text{val}}=-3.54 \text{ MeV}$), was selected and purified from the scattered primary ^{15}N beam and other contaminant nuclei by mean of several optical elements: a 30° -bending magnet, a Wien-filter, two quadrupole triplets and several collimators. Two parallel plate avalanche counters (PPACs) [14] were placed downstream prior to the beam entering the scattering chamber. The PPACs were utilized for on-line monitoring of the secondary ^{15}O beam profile, to provide an event-by-event reconstruction of the trajectory of the beam and for timing purposes. Finally, ^{15}O beam entered the the scattering chamber filled with ^4He gas at a pressure of 467 mbar, that was separated from the high vacuum beam line by a $2.2 \mu\text{m}$ thick Havar window. The ^{15}O beam intensity was in the range $1\text{-}2 \times 10^4$ particles/s with $\approx 99\%$ purity. The ^4He gas pressure and the temperature were continuously monitored by two capacitance manometers with an accuracy of 0.3% and a thermocouple device with 0.1 K sensitivity. The detection apparatus, illustrated in Fig. 1, consisted of two Double-Sided Silicon Strip Detectors (DSSSDs) from the EXPADES detector array [14]. The detectors were placed, the first at 0° and the second off 0° as shown in figure 1.

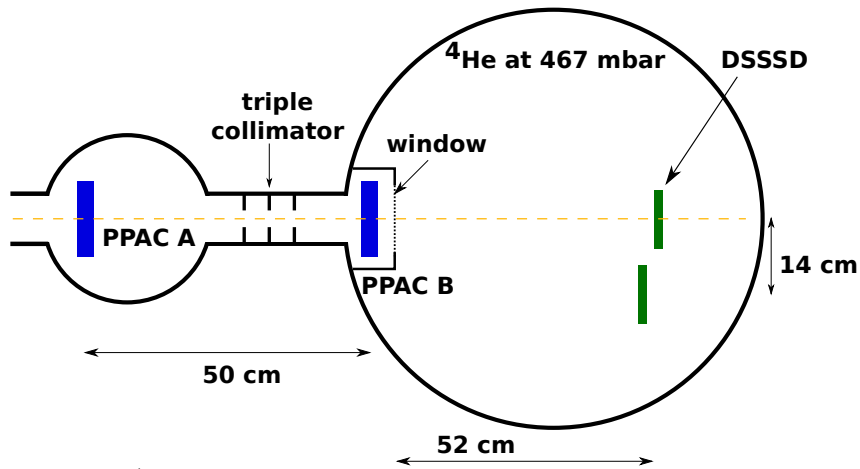


Figure 1. (color online) Schematic view of the experimental apparatus. The detection system consisted of two DSSSDs and two PPACs required for the time-of-flight measurement and beam tracking.

3. Data Analysis

The goal of the analysis is the reconstruction of the elastic scattering excitation function from the energy of the detected α -particles and their impact point on the detectors. The data coming from the two detectors were divided into three angular ranges. The first one corresponding to the whole detector placed at 0° while the detector off 0° was divided in two angular ranges.

The first step is the identification of α -particles produced in elastic scattering events. This was performed through measurements of the time-of-flight between the entering of the particle in the scattering chamber and the following recoiling particle on a DSSSD.

The final results are summarized in Fig. 2 showing the three excitation functions obtained from the two detectors, all three reveal the presence of resonances. Unfortunately the elastic scattering excitation functions corresponding to the detector off 0° have low statistics and very low resolution. This is mainly due to the fact that the effects of the energy and angular spread of the beam profile are larger for particles that are scattered at larger angles. Moreover due to the low statistics obtained for the detector off 0° the angular range is relatively high and this can be a further cause of resolution worsening. Due to the low statistics and low resolution the data at larger angle were not used in the R-matrix calculation (see section 4) for the identification of the spins and parities of the resonances observed in the elastic scattering excitation function.

4. Results and Conclusions

In order to determine the main properties of the observed resonances: widths, partial decay branches, energies and spins, an R -matrix calculation was performed. A comprehensive description of the R -matrix theory can be found in Ref. [15]. A full R -Matrix fit was performed using AZURE2 [16] which uses the Brune transformation. This was done for 0° ($\theta_{cm} = 180^\circ$). The statistics at the other angles were too poor to provide any constraint to the fit. Instead, the spins and energies of states from the mirror nucleus, ^{19}F [17], were used as a starting point for the fit; a powerful technique, with a good agreement between the energy levels in each nucleus. A two channel calculation were performed to fit the data: $^{15}\text{O}(\frac{1}{2}^-) + \alpha(0^+)$ and $^{18}\text{F}(1^+) + p(\frac{1}{2}^+)$, with channel radii for the i^{th} decay channel, $r_i = r_0(A_{recoil}^{\frac{1}{3}} + A_i^{\frac{1}{3}})$. and $r_0 = 1.4$ fm. Levels in the 5.3 – 8.9 MeV excitation-energy region have been investigated, with a number of newly observed states in this work. Furthermore, partial widths have been extracted for the observed levels, for many of them it is the first time measure-width data has been available. Reliable cross sections have been measured across the full range of levels populated representing important input to reaction-rate models.

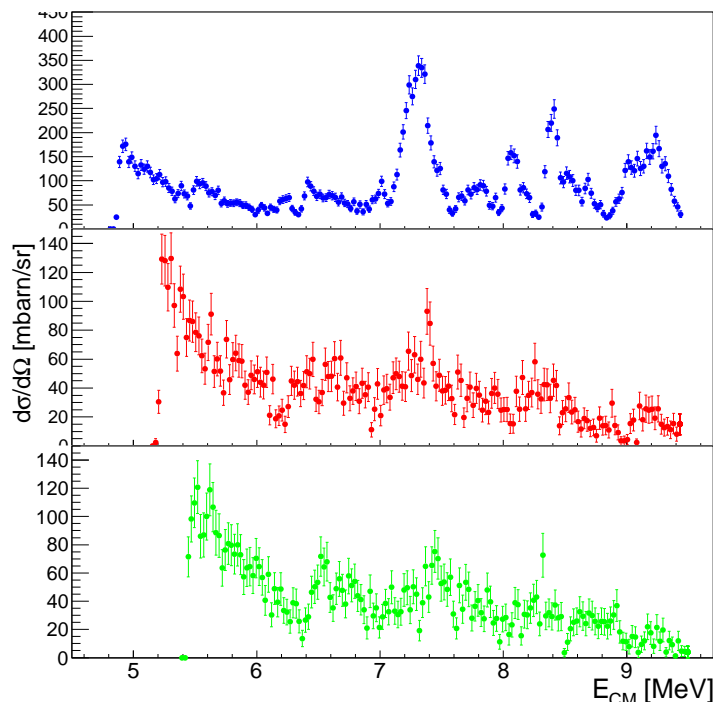


Figure 2. Elastic scattering excitation function for $^{15}\text{O}+^4\text{He}$ at the three different angular values: from top to down $\sim 180^\circ$, $\sim 160^\circ$, $\sim 155^\circ$

Acknowledgments

The present work has received funding from the European Unions Horizon 2020 research and innovation programme under the Marie Skłodowska-Curie grant agreement No 659744. The UK STFC is acknowledged for providing funding under grant ST/L005751/1. M.Z. was partially supported by the Croatian Science Foundation under Project No. 7194.

References

- [1] Wiescher M *et al* 2007 *Prog. Part. and Nucl. Phys.* **59** 51
- [2] Bardayan D W *et al* 2015 *Phys. Lett. B* **751** 311
- [3] von Oertzen W 2001 *Eur. Phys. J. A* **11** 403
- [4] Freer M *Rep. Prog. Phys.* **70** 2149
- [5] von Oertzen W, Freer M and Kanada-En'yo Y 2005 *Phys. Rep.* **432** 43
- [6] Thummerer S *et al* 2003 *J. Phys. G* **29** 509
- [7] Wheldon C *et al Eur. Phys. J. A* **26** 321
- [8] Artemov K P *et al* 1990 *Sov. J. Nucl. Phys.* **52** 634
- [9] Kallman K *et al* 1994 *Nucl. Instr. and Meth. in Phys. Res. A* **338** 413
- [10] Zadro M *et al* 2007 *Nucl. Instr. and Meth. in Phys. Res. B* **259** 836
- [11] Maidikov V Z *et al.* 2004 *Nucl. Phys. A* **746** 389c
- [12] Mazzocco M *et al* 2013 *Nucl. Instr. and Meth. in Phys. Res. B* **317** 223
- [13] Torresi D, Wheldon C *et al* 2014 *LNL Annual Report 19*, see http://www.lnl.infn.it/~annrep/read_ar/2014/contributions/pdfs/019_A_61_A056.pdf
- [14] Pierroutsakou D *et al*, submitted to *Nucl. Instr. and Meth. in Phys. Res. A*
- [15] Lane A M and Thomas R G 1958 *Reviews of Modern Physics* **30** 257
- [16] Azuma R *et al* 2010 *Phys. Rev. C* **81** 045805
- [17] Tilley D R, Weller H R, Cheves C M and Chasteler R M 1995 *Nucl. Phys. A* **595** 1